Synthesis and investigation of novel 6-(1,2,3-triazol-4-yl)-4-aminoquinazolin derivatives possessing hydroxamic acid moiety for cancer therapy

Chao Ding, Shaopeng Chen, Cunlong Zhang, Guangnan Hu, Wei Zhang, Lulu Li, Yu Zong Chen, Chunyan Tan, Yuyang Jiang

PII: S0968-0896(16)30915-4
DOI: http://dx.doi.org/10.1016/j.bmc.2016.10.006
Reference: BMC 13333

To appear in: *Bioorganic & Medicinal Chemistry*

Received Date: 21 July 2016
Revised Date: 6 October 2016
Accepted Date: 7 October 2016

Please cite this article as: Ding, C., Chen, S., Zhang, C., Hu, G., Zhang, W., Li, L., Chen, Y.Z., Tan, C., Jiang, Y., Synthesis and investigation of novel 6-(1,2,3-triazol-4-yl)-4-aminoquinazolin derivatives possessing hydroxamic acid moiety for cancer therapy, *Bioorganic & Medicinal Chemistry* (2016), doi: http://dx.doi.org/10.1016/j.bmc.2016.10.006

Synthesis and investigation of novel 6-(1,2,3-triazol-4-yl)-4-aminoquinazolin derivatives possessing hydroxamic acid moiety for cancer therapy

Chao Ding[a,b], Shaopeng Chen[b], Cunlong Zhang[c], Guangnan Hu[d], Wei Zhang[a,b], Lulu Li[b], Yu Zong Chen[c], Chunyan Tan[a,b,*], Yuyang Jiang[b,e,*]

[a] Department of Chemistry, Tsinghua University, Beijing 100084, PR China

[b] The State Key Laboratory Breeding Base-Shenzhen Key Laboratory of Chemical Biology, the Graduate School at Shenzhen, Tsinghua University, Shenzhen 518055, P. R. China

[c] Shenzhen Technology and Engineering Laboratory for Personalized Cancer Diagnostics and Therapeutics, Shenzhen Kivita Innovative Drug Discovery Institute, Shenzhen 518055, P. R. China

[d] Department of Medicine, University of Massachusetts Medical School, Worcester, Massachusetts 01605

[e] School of Medicine, Tsinghua University, Beijing 100084, PR China

* Corresponding author. Tel.: +86 755 2603 2094; fax: +86 755 2603 2094;
Email address: jiangyy@sz.tsinghua.edu.cn; tancy@sz.tsinghua.edu.cn

Abstract

By merging the critical pharmacophore of EGFR/HER2 and HDAC inhibitors into one compound, a novel series of EGFR, HER-2, and HDAC multitarget inhibitors were synthesized. Compounds **9a-l** contained 4-anilinoquinazolines with C-6 triazole-linked long alkyl chains of hydroxamic acid and displayed excellent inhibition against these enzymes (compound **9d** exhibited the best inhibitory potency on wild-type EGFR, HDAC1, and HDAC6 with IC_{50} values 0.12 nM, 0.72 nM and 3.2 nM individually). Furthermore, compounds **9b** and **9d** potently inhibited proliferation of five human cancer cell lines (with IC_{50} values between 0.49-8.76 μM). Further mechanistic study revealed that compound **9d** also regulated the phosphorylation of EGFR and HER2 and histone H3 hyperacetylation on the cellular level and induced remarkable apoptosis in BT-474 cells. Therefore, our study suggested that a system network-based multi-target drug design strategy might provided an alternate drug design method, by taking into account the synergy effect of EGFR, HER-2 and HDAC.

Keywords: EGFR; HER2; HDAC; multitarget; synergy; resistance.

1. Introduction

The ErbB tyrosine kinase family consists of four closely related members: epidermal growth factor receptor (EGFR, or ErbB1/HER1), human epidermal growth factor receptor 2 (HER2, or ErbB2/Neu), HER3 (ErbB3), and HER4 (ErbB4).[1] Binding ligands to the receptors stimulates ErbB dimer formation through homodimerization or heterodimerization, which triggers autophosphorylation of the receptor on a number of tyrosine residues.[2] Subsequently, this leads to the recruitment of appropriate adaptor or signaling proteins with SRC homology 2 (SH2) domains,[3] resulting in activation of several downstream pathways, such as the Ras/Raf/Erk[4] and PI3K/Akt/mTOR[5] pathways involved in the proliferation and survival response. Selective disruption of EGFR and HER2 by monoclonal antibodies and small-molecule inhibitors has been clinically validated as a rational strategy for cancer therapy.[6] As the first generation small-molecule EGFR inhibitors, gefitinib (ZD1839) and erlotinib (OSI-774) have markedly improved the overall survival (OS) of EGFR activating mutation (L858R and deletions in exon 19) in non-small cell lung cancer (NSCLC) patients.[7,8] Unfortunately, these inhibitors lack prolonged effectiveness due to acquired resistance mainly caused by T790M mutation at the gatekeeper and activation of alternative compensatory signaling pathways.[9-11] Second generation EGFR inhibitor, afatinib (BIBW-2992),[12] and third generation EGFR inhibitor, osimertinib (AZD9291),[13] have been approved by the U.S. FDA for the treatment of advanced NSCLC in patients with T790M mutation. However, the resistance caused by upregulation of bypass signal, which consists of numerous

genetic and epigenetic signaling aberrations including MET amplification, PIK3CA mutation, BRAF mutation, etc., is still a major problem facing current cancer research.[9,14,15]

Several strategies have been proposed to overcome the limitation of concurrent activation of other bypass pathways.[10,16] One promising approach is to disrupt multiple pathways by the inhibition of histone deacetylase (HDAC). HDAC can remove acetyl groups from histone and non-histone proteins, condense chromatin, and prevent gene transcription.[17] Modulation of activities of HDACs can impact the activity of a diverse range of proteins, including tubulin, p53, and Hsp90, which control a variety of cellular processes, such as cell cycle arrest, differentiation, and apoptosis.[18] In the past decade, much progress has been made in the development of HDAC small-molecule inhibitors. Vorinostat (SAHA), romidepsin (FK-228), and ponobinostat (LBH589) have been licensed by the U.S. FDA as treatments for cutaneous T cell lymphoma (CTCL) and multiple myeloma.[19-21]

Many studies have shown that there is synergistic crosstalk between EGFR/HER2 and HDAC.[22-24] Inhibition of HDAC6 leads to increased acetylation of Hsp90,[25] resulting in degradation of a number of Hsp90 client proteins that play important roles in cancer cell proliferation, such as mut-EGFR, HER2, AKT, c-Raf, and ABL.[26,27] HDAC6 inhibitors could act in the similar manner as Hsp90 inhibitors. Moreover, HDAC inhibitors can alter gene expression, increase production of reactive oxygen species (ROS), and induce cell cycle arrest, etc.,[18] which may also indirectly contribute to the anti-cancer activity of EGFR/HER2 inhibitors. It is reported that

treatment with vorinostat or panobinostat led to increased Hsp90 acetylation, EGFR/HER2 degradation, cell death, and synergized with ErbB inhibitors, such as erlotinib, lapatinib, or trastuzumab in EGFR/HER2 over-expressed cancer cell lines. Thus, targeting EGFR/HER2 and HDAC simultaneously might offer benefits for cancer therapy.[22-24]

Recently, several studies have reported on EGFR/HDAC dual inhibitors and yielded satisfactory results.[28-29] One of the most potent compounds, CUDC-101 (7-(4-(3-Ethynylphenylamino)-7-methoxyquinazolin-6-yloxy)-N-hydroxyheptanamide, **9**, Figure 1), which possesses an oxygen atom as a linker between the pharmacophore of HDAC inhibitors (hydroxamic acid) and the pharmacophore of EGFR inhibitors (4-phenyl-aminoquinazoline), has already entered Phase I clinical investigation.[30] In this study, we utilized a 1,2,3-triazole as a linker between hydroxamic acid and 4-phenylamino-quinazoline. 1,2,3-triazole is relatively resistant to metabolic degradation and is exceedingly stable in acidic/basic and reductive/oxidative conditions, suggesting that it could be used to improve pharmacokinetic properties of the desired drugs.[31] Further, triazoles may also be capable of participation in generating functional bioisosteres to substitute esters and amides.[32] Due to these desirable features of this moiety, 1,2,3-triazole has been widely employed by medicinal chemists in drug discovery processes. In this study, we would report a novel series of EGFR/HER2/HDAC multitarget inhibitors with 1,2,3-triazole as the linker, which have potential for cancer therapy.

(**Figure 1** should be listed here)

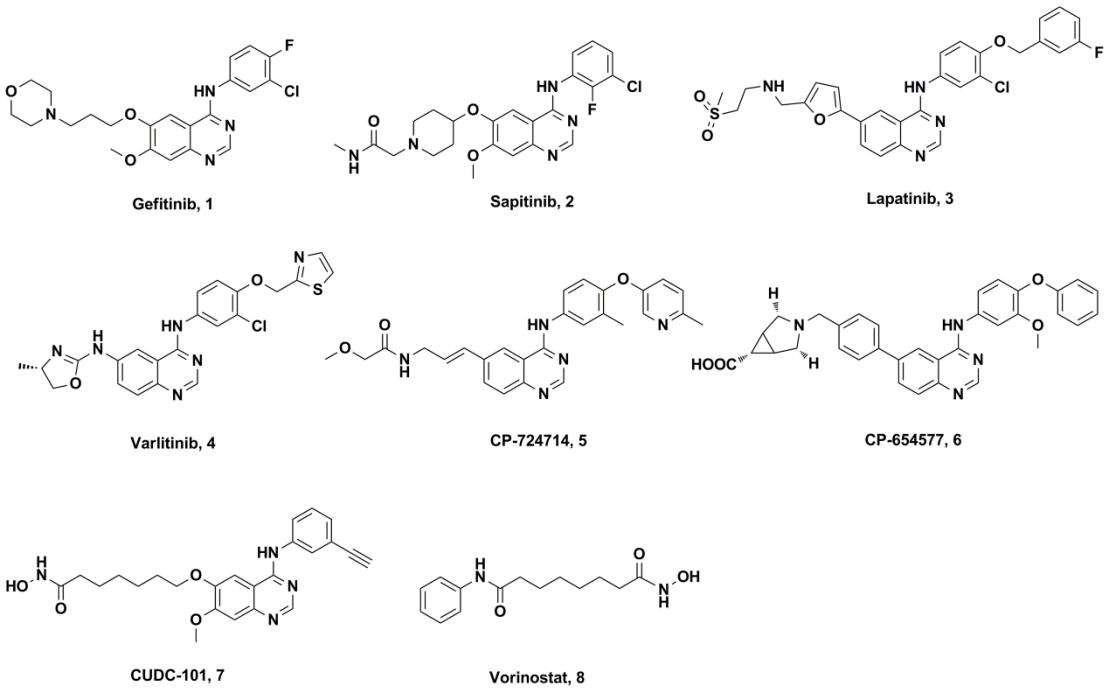

Figure 1. Selected quinazoline-based EGFR/HER2 inhibitors **1-6**, EGFR/HER2/HDAC multitarget inhibitor **7** and HDAC inhibitor **8**.

2. Design

Among known drugs in clinical use or in clinical trials, 4-aminoquinazoline is the most common scaffold of selective EGFR and HER2 inhibitors. As shown in the X-ray cocrystal structures of EGFR/HER2 with selective EGFR inhibitor gefitinb (**1**)[33] and dual EGFR/HER2 inhibitor lapatinib (GW-572016, **3**),[34] the quinazoline moiety occupies the adenine region of the ATP-binding pocket and forms a hydrogen bond with Met793 (EGFR) or Met801 (HER2) in the hinge at N1 of quinazoline, while the phenyl-amino group fits into the hydrophobic BP-I and BP-II pockets. Substituent at C-6 of the quinazoline core extends towards the hydrophilic E_1 region, which could be utilized to improve the pharmacokinetic properties and cellular activity.[35] These key features are also applied to other ErbB inhibitors, such as dual EGFR/HER2 inhibitors, sapitinib (AZD-8931, **2**) and varlitinib (ARRY-334543, **4**),

selective HER2 inhibitors CP-724714 (**5**) and CP-654577 (**6**) (Figure 1). Since the C-6 substituent is primarily composed of a hydrophilic part *via* a flexible linker, such as furyl, phenyl, or vinyl, we decided to modify this substituent with a triazole linker, which can mimic the direction of the hydrophilic part without dramatically hampering EGFR activity.

Meanwhile, co-crystals of HDACs bound with vorinostat (**8**)[36] revealed common binding modes between HDAC and HDAC inhibitors. (1) A cap group, which is a hydrophobic group, recognizes the surface outside the HDAC active pocket. (2) A linker that can extend to a certain distance leads to the active site. 3) A zinc-binding group (ZBG) directly interacts with the zinc ion at the conserved active site. Based on the structure of vorinostat, we retained the hydroxamic acid functional group as ZBG and maintained a chain length of five or six carbons (which can exhibit the best potency against HDAC). However, we replaced the phenyl group with other hydrophobic groups and used triazole instead of amide since they are bio-isosterisms in drug design. It is validated that the preference of the cap group is quite flexible in which variation of this group to a certain extent would not dramatically affect the binding to HDAC.

Given the above analysis of key determinants for the functional pockets and molecular recognition of EGFR and HDAC, we merge the critical pharmacophore of EGFR/HER2 inhibitors and HDAC inhibitors into one compound. As depicted in Scheme 1, the 4-aminoquinazoline of compounds **9a-9l** interacted with EGFR and HER2 with high potency and selectivity. Meanwhile, the introduction of a long alkyl

chain of hydroxamic acid reached the active site and chelated zinc to inhibit HDAC enzyme activity. Therefore, compounds **9a-9l** may be able to interact with EGFR, HER2, and HDAC independently and thus block multiple signaling pathways simultaneously.

(**Scheme 1** should be listed here)

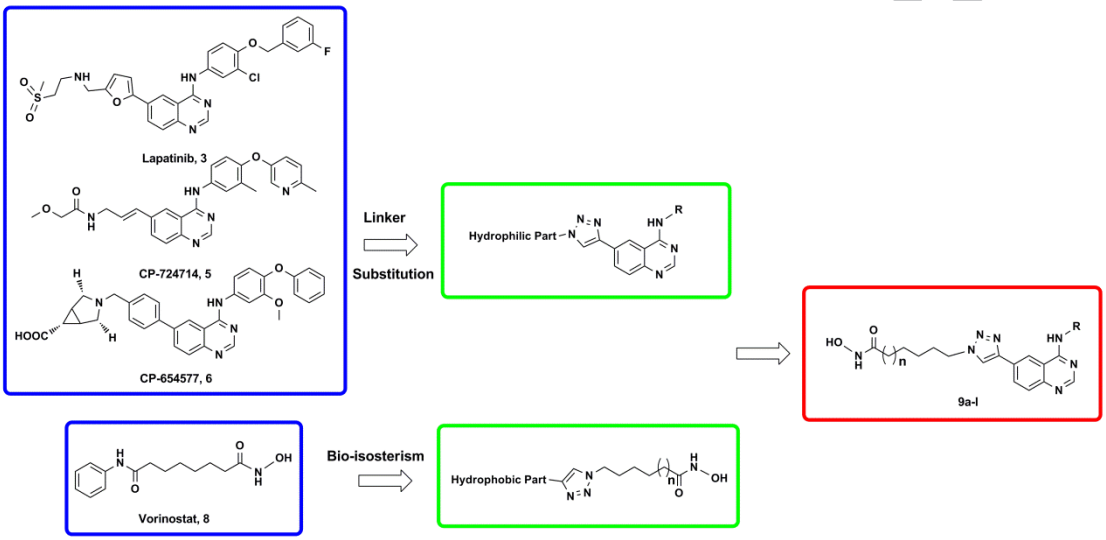

Scheme 1. Design strategy of novel EGFR/HER2/HDAC multitarget inhibitors.

3. Chemistry

Compounds **9a-l** were synthesized according to Scheme 2. The key intermediate **12** was generated from commercially available compound **10** *via* cyclization and chlorination. Coupling anilines with **12** produced compounds **13a-f**. Compounds **15a-f** were prepared through a classical Sonogashira reaction and deprotection. The key intermediates **18a** and **18b** were obtained from commercially available compounds **16a** and **16b** respectively via azidation and amidation. Coupling **15a-f** with 18a-b followed by acidification afforded the final products **9a-l**.

(**Scheme 2** should be listed here)

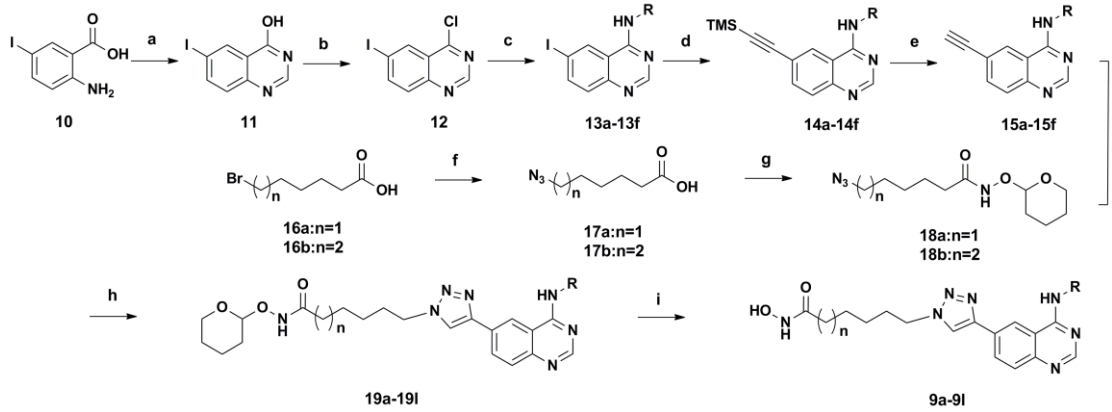

Scheme 2. Reagents and conditions: (a) NH_2CHO, reflux; (b) $SOCl_2$, DMF(cat), reflux; (c) anilines, iso-PrOH, 80°C; (d) trimethylsilylacetylene, $Pd(PPh_3)_2Cl_2$, CuI, THF/Et_3N, 80°C; (e) TBAF, THF, RT; (f) NaN_3, DMF, 80°C; (g) NH_2OTHP, EDCI, DMAP, $CHCl_3$, RT; (h) $CuSO_4 \cdot 5H_2O$, sodium ascorbate, DMF, 60°C; (i) HCl, dioxane, RT.

4. Results and discussion

4.1. *In vitro* enzyme inhibition

We first tested the inhibitory activity of the target compounds against EGFR, HER2, and HDAC enzymes using gefitinib, lapatinib, and vorinostat as the positive control compounds (Table 1). We were pleased to find that almost all compounds strongly inhibited EGFR, HDAC1, and HDAC6 with potencies comparable to that of selective EGFR inhibitor gefitinib and HDAC inhibitor vorinostat. 8 compounds also exhibited outstanding to moderate inhibitory activity on HER2 with IC_{50} values less than 1 μM. Among the 8 compounds, compounds **9c** and **9d** displayed the best potencies on EGFR and HDAC. For instance, compound **9d** strongly suppressed the wild-type EGFR and HDAC1 with IC_{50} values in subnanomolar ranges (0.12 nM for EGFR and 0.72 nM for HDAC1) and inhibited HDAC6 with IC_{50} value in single-digit

nanomolar range (3.2 nM), which is 3-80 fold more potent than gefitinib (9.6 nM for EGFR) and vorinostat (12 and 11 nM for HDAC1 and HDAC6).

(**Table 1** should be listed here)

Table 1 Enzymatic inhibitory activities of compounds **9a-9l** against EGFR, HER2, HDAC1, and HDAC6.[a]

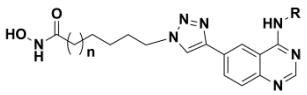

9a-9l

Compd	R	n	EGFR (IC50, nM)	HER-2 (IC50, nM)	HDAC1 (IC50, nM)	HDAC6 (IC50, nM)
9a		1	0.65 ± 0.08	165.5 ± 21.6	7.0 ± 0.6	9.5 ± 0.8
9b		2	0.69 ± 0.12	176.7 ± 10.4	2.6 ± 0.4	8.4 ± 1.2
9c		1	0.27 ± 0.04	386.1 ± 25.7	1.4 ± 0.1	4.1 ± 1.4
9d		2	0.12 ± 0.03	174.9 ± 19.6	0.72 ± 0.11	3.2 ± 0.5
9e	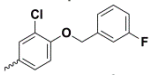	1	1.9 ± 0.4	192.8 ± 25.1	38.6 ± 4.5	94.2 ± 12.6
9f	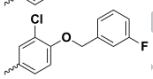	2	4.2 ± 0.3	16.4 ± 0.9	8.3 ± 0.7	19.5 ± 1.1
9g	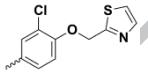	1	6.9 ± 1.2	537.4 ± 34.6	7.2 ± 2.5	14.3 ± 2.2
9h	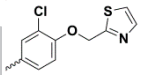	2	3.6 ± 0.5	706.7 ± 109.5	5.6 ± 0.9	13.6 ± 0.9
9i	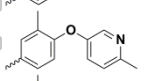	1	6.4 ± 0.5	>1000	6.9 ± 0.4	12.9 ± 4.3
9j	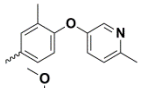	2	10.0 ± 1.7	>1000	5.2 ± 1.8	13.8 ± 1.6
9k	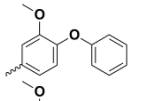	1	5.8 ± 1.2	>1000	26.6 ± 3.4	18.5 ± 3.3
9l	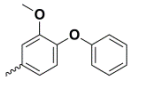	2	11.6 ± 0.9	>1000	12.8 ± 2.5	16.0 ± 1.9
Gefitinib		-	9.6 ± 0.7	NT[b]	NT	NT
Lapatinib		-	NT	23.9 ± 1.4	NT	NT
Vorinostat		-	NT	NT	10.8 ± 1.4	10.8 ± 0.7

[a] All the results were obtained from 2 different assays. [b] NT means not tested.

Next, we investigated the influence of chain length and substituents of the 4-amino group on the inhibition of enzymes. We first evaluated the influence of chain

length on the inhibition of EGFR, HER2, and HDAC. The data suggest that EGFR and HER2 inhibitions were largely unaffected by the change in carbon chain length (basically less than 2-fold increase, or loss of activity was observed between the 5-carbon chain length compounds (n=1) and the respective 6-carbon chain length compounds (n=2)) with the exception of compound **9f**, which had a 10-fold enhancement of activity in inhibiting HER2 compared to compound **9e** (192.8 nM vs. 16.35 nM). Since the triazole-linked long alkyl chains of hydroxamic acid extends towards the hydrophilic E_1 region, one carbon chain length difference is not expected to significantly affect the potency of EGFR and HER2.[35] Meanwhile, almost all 6-carbon chain length compounds displayed better potencies than the respective 5-carbon chain length compounds against both HDAC1 and HDAC6, which is congruent with previous reports.[30] Our next step was to examine the influence of the phenyl ring on the inhibition of EGFR, HER2, and HDAC. Although the ATP binding pockets of EGFR and HER2 have high degree of similarity, it is reported that different 4-anilino functional groups can alter the selectivity between EGFR and HER2.[37] Usually, small aniline substituted quinazolines such as gefitinib tend to be strong inhibitors of EGFR and moderate inhibitors of HER2.[38] As the aniline motifs become larger, these quinazoline derivatives such as lapatinb and varlitinib exhibit enhanced potency against HER2.[39,40] By replacing the aniline 4-position with large lipophilic phenyl ether, such as in CP-724714 and CP-654577,[41,42] the inhibition on EGFR is abolished, and these compounds become selective HER2 inhibitors (Table S1). Here, we compared the changes in potency and selectivity of the newly synthesized

compounds to the original compounds **1-6** against EGFR and HER2. Our results suggest that the introduction of a vorinostat-like segment to quinazoline basically improved the inhibition of EGFR but reduced the inhibition of HER2, thus, the selectivity profiles changed dramatically. For example, sapitinib, lapatinib, and varlitinib are dual inhibitors of EGFR and HER2, but **9c-h** which bearing the respective 4-anilino functional groups displayed more than 100-fold selectivity between EGFR and HER2 (with the exception of compound **9f**). Similar trends were also observed in **9i-l** in which the potencies on HER2 nearly diminished, and these four compounds have become EGFR selective inhibitors. These unexpected effects may result from the introduction of triazole linked long alkyl chains of hydroxamic acid. It seems that substituents at C-6 of the quinazoline not only affect the pharmacokinetic properties and cellular activity, but also have an obvious influence on the activity and selectivity of EGFR and HER2. Different from EGFR/HER2 inhibition, 4-anilino functional groups are not critical for selectivity for HDAC interaction. However, the substituted groups on the phenyl ring had a significant impact on the activities of HDAC inhibition. With increasing size of the substituted groups, the potencies on HDAC decreased markedly. This might be due to the fact that the substituted groups on the phenyl ring could form steric clash to affect their potential interaction with the active pocket of HDAC. For instance, Compounds **9a-9d**, which have the smallest substituents on the phenyl ring, displayed the best potencies of HDAC inhibition (IC_{50} less than 10 nM). Compounds **9g-9l**, which possess bigger substituents on the phenyl ring, inhibited the HDAC6 with IC_{50} values

between 10-20 nM. Not surprisingly, compounds **9e** and **9f**, with the biggest 3-fluorophenylmethoxy group at 4-position of aniline, displayed the weakest potencies of HDAC inhibition.[30]

4.2. Cytotoxity studies

We next determined the anti-proliferative effects of the synthetic compounds using an MTT assay against A549 cells (EGFR overexpressed, k-Ras mutation) and BT-474 cells (HER2 overexpressed) with lapatinib and vorinostat as the positive control compounds. As shown in Table 2, most of the compounds suppressed the growth of two cancer cells with IC_{50} values in the micromolar range. Almost all 6-carbon chain length compounds displayed better efficacies than the respective 5-carbon chain length compounds against both cells. It is worthy to note that **9b** and **9d**, with small substituents on the phenyl ring, which may possess the better cell membrane permeability and lower molecule weights, inhibited the proliferation of A549 cells more effectively than lapatinb and vorinostat (with IC_{50} values 0.51 and 0.63 μM respectively). However, the cellular activities against BT-474 cells were largely unaffected by the changes in phenyl ring substitution. Since most compounds showed moderate to weak inhibition of HER2, the inhibition of EGFR and HDAC may contribute largely to the their anti-proliferative effects against BT-474 cells.[24]

(**Table 2** should be listed here)

Table 2 Cellular inhibitory activities of compounds **9a-9l** against A549 and BT-474 cells. [c]

Compd	A549 (IC50, μM)	BT-474 (IC50, μM)	Compd	A549 (IC50, μM)	BT-474 (IC50, μM)
9a	>50	26.01 ± 1.51	**9h**	8.79 ± 0.61	2.88 ± 0.26
9b	0.51 ± 0.04	3.63 ± 0.31	**9i**	8.46 ± 0.89	14.65 ± 1.02

9c	>50	>50	**9j**	16.53 ± 0.95	4.41 ± 0.42
9d	0.63 ± 0.12	3.88 ± 0.06	**9k**	43.45 ± 3.68	23.61 ± 1.28
9e	>50	2.20 ± 0.20	**9l**	13.49 ± 0.23	4.95 ± 0.24
9f	3.68 ± 0.55	2.24 ± 0.13	Lapa[d]	1.74 ± 0.28	0.10 ± 0.02
9g	9.96 ± 0.56	20.64 ± 1.21	Saha[e]	2.57 ± 0.37	2.67 ± 0.38

[c] The values are the average of three independent experiments run in triplicate. [d] Lapa means lapatinib,[e] Saha means vorinostat.

Given the excellent enzymatic and cellular activities and related "drug-like" characteristics of **9b** and **9d** (with lowest molecule weights which could be more closed to meet the rule of 5), we next tested their anti-proliferative effects on three other cancer cell lines with varying levels of EGFR and HER2-A431 (EGFR overexpressed), SK-BR-3 (HER2 overexpressed), and NCI-H1975 (EGFR T790M/L858R) in order to determine if these compounds could exhibit broad and balance antitumor activities against solid tumor cells. As shown in Table 3, both **9b** and **9d** possessed modest to high level of inhibitory activities against these cell lines. Anti-proliferative effects of **9b** and **9d** on A431 and SK-BR-3 cells are similar to those against A549 and BT-474 cells. Compounds **9b** and **9d** inhibited A549 and A431 (EGFR inhibitor sensitive) cells with potencies comparable to that of lapatinib, but suppressed BT-474 and SK-BR-3 (HER2 inhibitor sensitive) cells much less potently than lapatinib. The difference of potencies on HER2 between compounds **9b, 9d** and lapatinib (176.7 and 174.9 versus 23.9 nM) may well explain why lapatinib exhibited a better anti-proliferative effect than compound **9b** and **9d** against these two breast cancer cell lines. Compounds **9b** and **9d** also modestly inhibited NCI-H1975 cells with potencies comparable to that of lapatinib (with IC_{50} values 8.76, 8.05 and

7.85 μM respectively). It is reported that compared to wild-type EGFR selective inhibitors, such as gefitinib and erlotinib, NCI-H1975 (EGFR T790M/L858R mutated) cells are more sensitive to dual EGFR/HER2 inhibitor lapatinib, which could block the heterodimerization of EGFR and HER2 by HER2 inhibition. In this study, compound **9d** inhibited HER2 less potently than lapatinib. However, the inhibition on HDAC may compensate the anti-proliferative effect of **9d** in a certain extent against NCI-H1975 cell line, although both **9d** and lapatinib are not able to overcome the resistance caused by EGFR T790M mutation. The anti-proliferative data provide further evidence that the synthetic compounds may exhibit broad antitumor activities through inhibiting multiple targets, including EGFR, HER2, and HDAC pathways.

(**Table 3** should be listed here)

Table 3 Cellular inhibitory activities of the representative compounds **9b** and **9d** against A549, A431, BT-474, SK-BR-3, and NCI-H1975 cells.[f]

Compd	A549 (IC50, μM)	A431 (IC50, μM)	BT-474 (IC50, μM)	SK-BR-3 (IC50, μM)	NCI-H1975 (IC50, μM)
9b	0.51 ± 0.04	1.95 ± 0.13	3.63 ± 0.31	1.27 ± 0.22	8.76 ± 0.26
9d	0.63 ± 0.12	0.49 ± 0.06	3.88 ± 0.06	0.69 ± 0.03	8.05 ± 1.15
Lapatinib	1.74 ± 0.28	0.15 ± 0.01	0.10 ± 0.02	0.06 ± 0.01	7.25 ± 0.38
Vorinostat	2.57 ± 0.37	2.29 ± 0.04	2.67 ± 0.38	2.58 ± 0.13	1.90 ± 0.09

[f] The values are the average of three independent experiments run in triplicate.

4.3. Compound 9d blocks cellular EGFR and HER2 phosphorylation and induces histone H3 hyperacetylation

Given the highly potent inhibitory activity of synthetic compounds on enzymes and cancer cell lines, we further tested whether the compounds could inhibit the phosphorylation of EGFR and HER2 and induce histone H3 hyperacetylation on the

cellular level. Compound **9d** was selected for further experimentation. Exposing cells to **9d** led to an obvious suppression of EGFR phosphorylation and activation of H3 hyperacetylation in a dose-dependent manner in A549 cells (Figure 2A), with almost complete inhibition of p-EGFR (Tyr1068 and Tyr1173) observed at 0.5 μM and marked upregulation of histone H3 (Lys27) hyperacetylation at 2.5 μM. In addition, **9d** also moderately decreased the levels of HER2 phosphorylation in a dose-dependent manner in BT-474 cell lines (Figure 2B), with almost complete inhibition of p-HER2 (Tyr1248) at 1 μM and p-HER2 (Tyr1221/1222) at 25 μM, which is in consistent with the outstanding inhibitory activity on EGFR, HDAC and the moderate potency on HER2 of **9d**. These results show that **9d** displays activities in a variety of cancer cell types by co-targeting EGFR, HER2, and HDAC pathways.

(**Figure 2** should be listed here)

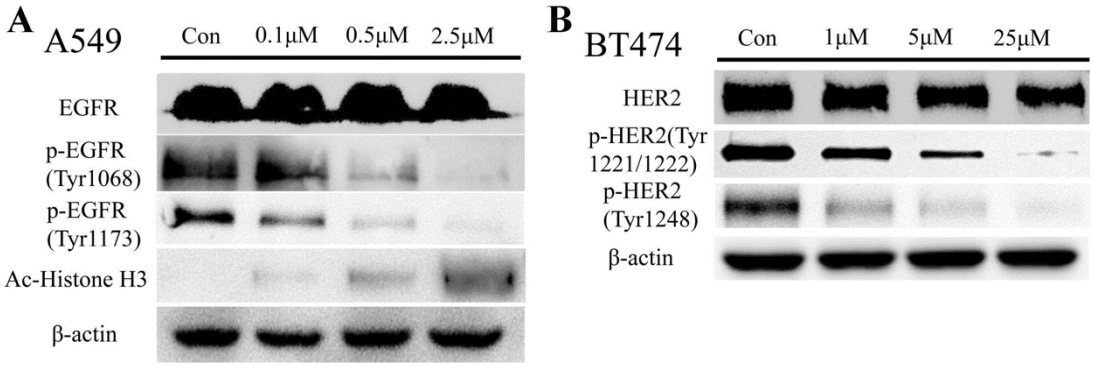

Figure 2. (A) Western blot analysis of A549 cells treated for 24 h with compound **9d**, (B) Western blot analysis of BT-474 cells treated for 24 h with compound **9d**.

4.4. Compound 9d induces apoptosis

To further dissect the growth-inhibitory effects of synthetic compounds, we evaluated the ability of **9d** to induce apoptosis in BT-474 cancer cells. We

characterized the proapoptotic activity of **9d** by flow cytometry. As shown in Figure 3, compound **9d** induced apoptosis in BT-474 cells in a concentration-dependent manner. Treatment in BT-474 cells with 5.0 uM **9d** resulted induced apoptosis in 63.86% of cells. This result suggests that **9d** is able to promote pronounced anti-proliferative and proapoptotic effects in BT-474 cells, which may result from concerted inhibition of EGFR, HER2, and HDAC activity.

(**Figure 3** should be listed here)

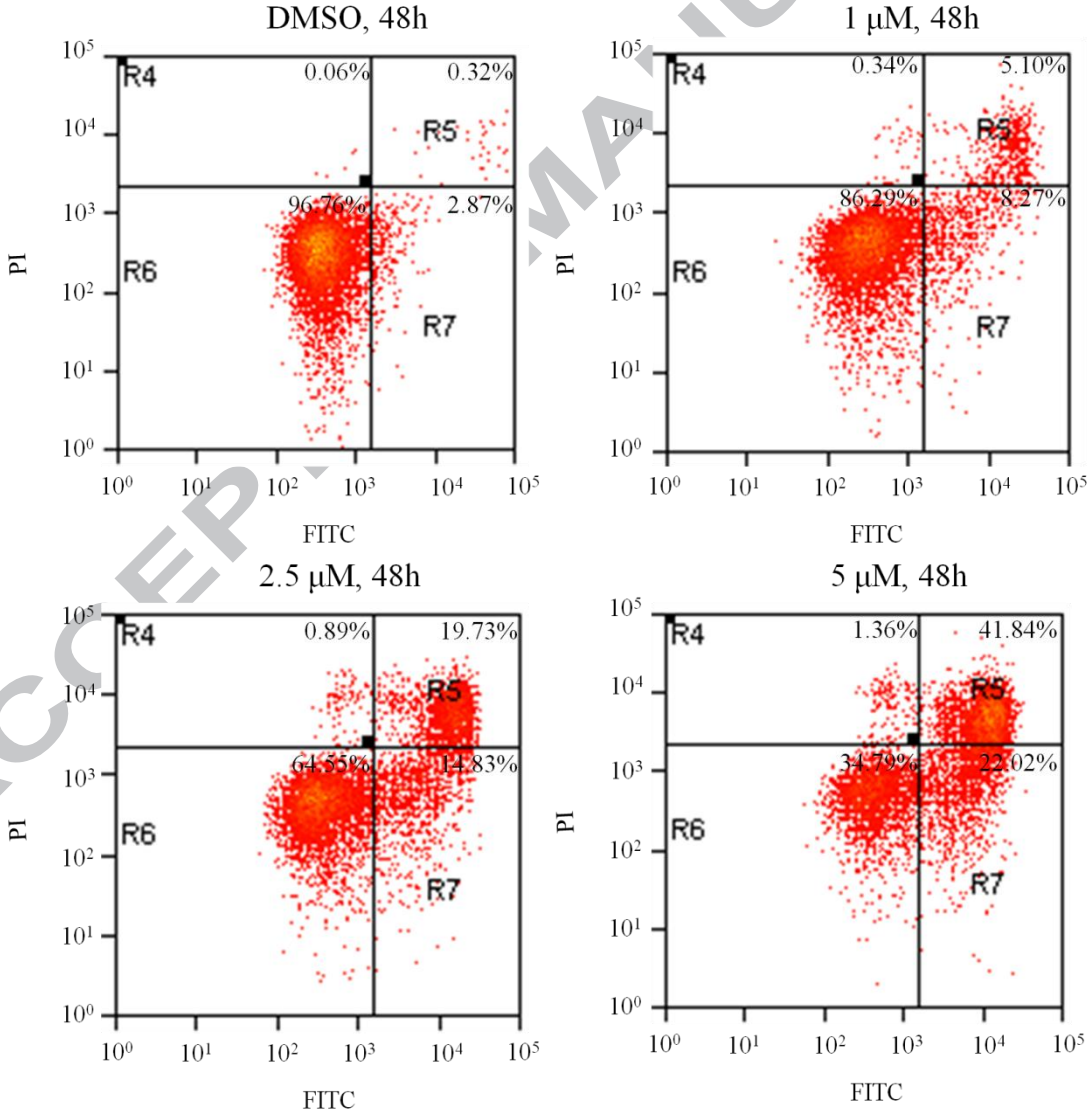

Figure 3. *In vitro* apoptosis analysis of **9d** in BT-474 cells.

4.5. Binding modes of compound 9d with EGFR and HDAC

To explore the binding modes of multitarget compounds with the respective enzymes, compound **9d**, which exhibited the best potency on EGFR and HDAC, was docked into active sites of EGFR (PDB ID code: 1XKK[34]) and HDAC2 (PDB ID code: 4LXZ[43]). Since the structure of HDAC2 (not HDAC1) crystallized with vorinostat has been solved, in this study, we chose HDAC2 which have identical active sites around the entrance of the channel with HDAC1 for molecular docking simulation study.[44]

The binding modes of compound **9d** with EGFR and HDAC2 were shown in Figure 4A and 4B. As depicted in Figure 4A, the N1 of quinazoline forms a hydrogen bond with Met793 in the hinge while the phenyl-amino group fits into the hydrophobic pockets of EGFR and the fluorine atom forms a hydrogen bond with Thr854. C-6 triazole-linked long alkyl chains of hydroxamic acid extends towards the hydrophilic region and the hydroxy group forms a hydrogen bond with Asp800. Figure 4B demonstrates that the 4-aminoquinazoline group occupies the surface outside the HDAC2 active pocket while the triazole-linked six carbons chain length extends to a proper distance thus leading the hydroxamic acid group to the active site and chelating with zinc. The hydroxamic acid group forms four hydrogen bonds with Tyr308, Asp181, His145, and His146. The above docking results may explain why compound **9d** showed the outstanding effective inhibitory activity against EGFR and HDAC.

(**Figure 4** should be listed here)

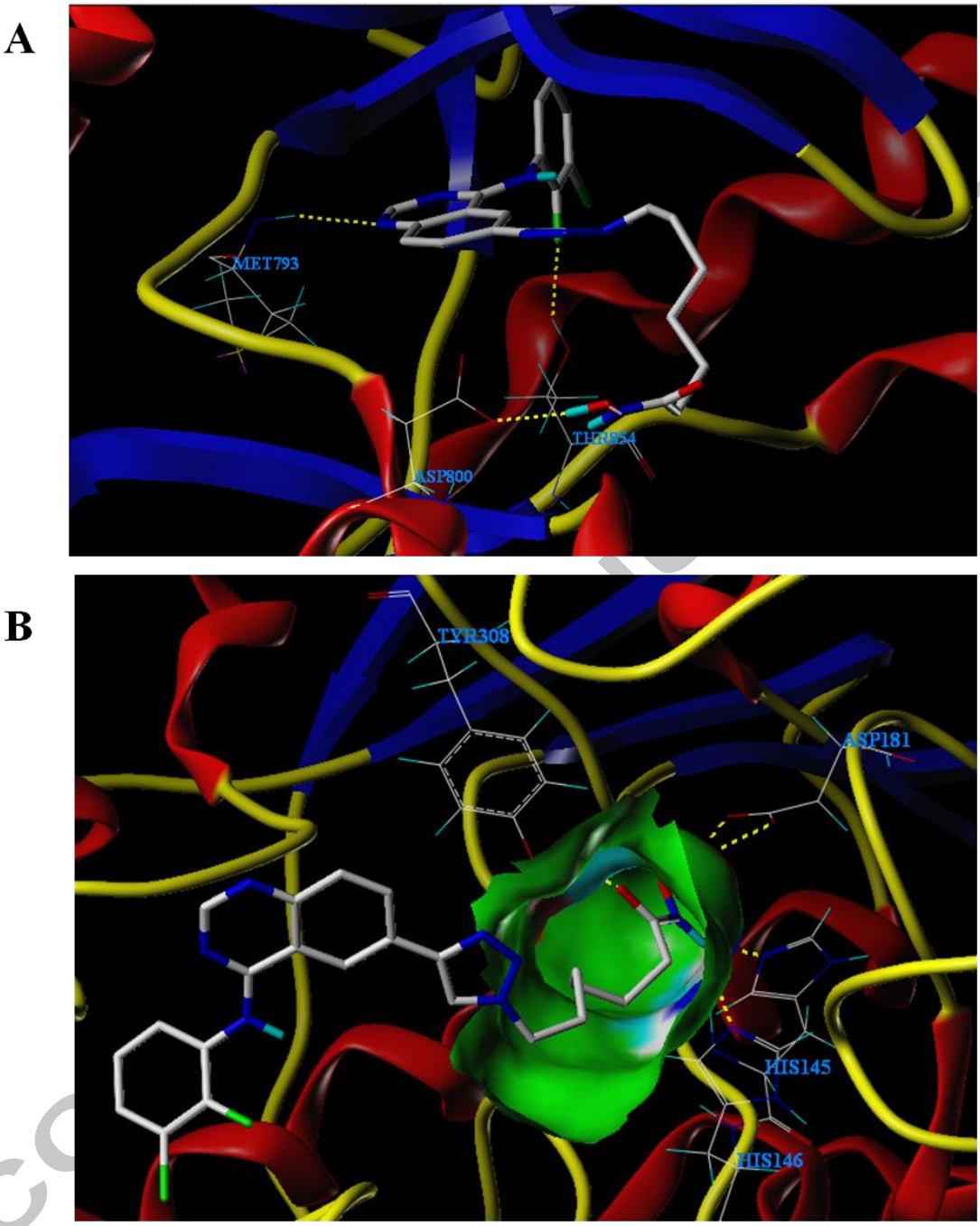

Figure 4. (A) Proposed binding mode of compounds **9d** with EGFR (1XKK), (B) Proposed binding mode of compounds **9d** with HDAC2 (4LXZ) (N and O atoms in blue and red, respectively). These images were generated using the SYBYL program.

5. Conclusion

A novel series of 4-anilinoquinazolines with C-6 triazole-linked long alkyl chains of hydroxamic acid were designed, synthesized, and evaluated as multitarget

EGFR/HER2/HDAC inhibitors. Most of the compounds displayed excellent inhibition against these enzymes. Furthermore, compounds **9b** and **9d** potently inhibited proliferation of five human cancer cells. Compound **9d** also obviously inhibited the phosphorylation of EGFR and HER2 and induced histone H3 hyperacetylation on the cellular level. Moreover, compound **9d** induced remarkable apoptosis in BT-474 cells. This system network-based[45-47] multitarget inhibition approach, which is able to simultaneously interact with multiple targets (also called polypharmacology), offers enhanced benefits compared to single-targeted therapies, including lower probability of developing resistance, larger therapeutic windows, and more durable responses.[16,48,49] This system also proves to minimize several liabilities of drug-drug combination approaches, including the less predictable pharmacokinetic profiles, the potential for additive or synergistic toxicities, possibilities of drug-drug interactions, poor patient compliance, and high treatment costs.[50,51] This work provides a novel approach to be considered for cancer therapies, acknowledging that polypharmacology has been gaining much attention in drug discovery and synthesis as of recent.[52-55]

6. Experimentals

6.1. Chemistry

The reagents (chemicals) were commercially available and used without further purification. Nuclear magnetic resonance spectra were obtained using a Bruker 400 (400 MHz) spectrometer using TMS as an internal standard. Chemical shifts were reported in a d (ppm) and spin – spin coupling constants as J (Hz) values. The mass

spectra were obtained on a Waters Micromass Q-TOF Premier Mass Spectrometer. Melting points were determined with a SGW X-4 digital apparatus, uncorrected and reported in degrees Centigrade.

6.1.1. General procedure for compounds 9a-l.

2 M HCl in dioxane (1 mL) was added dropwise to a solution of the **19a-l** intermediate (0.5 mmol) in dioxane (5 mL) and the mixture was stirred at room temperature for 1 h. The precipitate was filtered off, washed with ethyl ether, and dried to give the desired hydroxamic acid **9a-l**.

6.1.1.1. 6-(4-(4-((3-chloro-4-fluorophenyl)amino)quinazolin-6-yl)-1H-1,2,3-triazol-1-yl)-N-hydroxyhexanamide (9a) Yield 85%; mp 216-218°C; ^{1}H NMR (400 MHz, DMSO) δ 12.07 (s, 1H), 10.43 (s, 1H), 9.63 (s, 1H), 8.99 (s, 1H), 8.96 (s, 1H), 8.56 (d, J = 8.8 Hz, 1H), 8.12 (dd, J = 6.8, 2.5 Hz, 1H), 8.03 (d, J = 8.7 Hz, 1H), 7.85 (ddd, J = 8.8, 4.2, 2.7 Hz, 1H), 7.57 (t, J = 9.1 Hz, 1H), 4.46 (t, J = 7.0 Hz, 2H), 2.05 – 1.81 (m, 4H), 1.64 – 1.43 (m, 2H), 1.35 – 1.18 (m, 2H). ^{13}C NMR (101 MHz, DMSO) δ 169.41, 160.31, 156.98, 154.53, 151.29, 145.34, 138.75, 134.51, 134.48, 133.39, 131.71, 127.09, 125.84, 125.77, 123.40, 121.18, 119.79, 119.60, 117.50, 117.28, 114.63, 50.16, 32.51, 29.77, 25.92, 24.97. HR-MS(ESI) *m/z*: Calcd for $[M+H]^{+}$ 470.1508; Found: 470.1501.

6.1.1.2. 7-(4-(4-((3-chloro-4-fluorophenyl)amino)quinazolin-6-yl)-1H-1,2,3-triazol-1-yl)-N-hydroxyheptanamide (9b) Yield 94%; mp 228-230°C; ^{1}H NMR (400 MHz, DMSO) δ 12.06 (s, 1H), 10.40 (s, 1H), 9.62 (s, 1H), 8.99 (s, 1H), 8.95 (s, 1H), 8.56 (dd, J = 8.7, 1.3 Hz, 1H), 8.13 (dd, J = 6.8, 2.5 Hz, 1H), 8.03 (d, J = 8.7 Hz, 1H), 7.85

(ddd, *J* = 8.9, 4.3, 2.5 Hz, 1H), 7.58 (t, *J* = 9.1 Hz, 1H), 4.46 (t, *J* = 7.0 Hz, 2H), 2.03 – 1.75 (m, 4H), 1.56 – 1.40 (m, 2H), 1.36 – 1.20 (m, 4H). ^{13}C NMR (101 MHz, DMSO) *δ* 169.53, 160.30, 156.97, 154.52, 151.36, 145.35, 138.93, 134.55, 134.52, 133.40, 131.69, 127.07, 125.82, 125.75, 123.37, 121.14, 119.79, 119.61, 117.51, 117.29, 114.67, 50.24, 32.64, 29.96, 28.44, 26.07, 25.40. HR-MS(ESI) *m/z*: Calcd for $[M+H]^+$ 484.1664; Found: 484.1661.

6.1.1.3.

6-(4-(4-((3-chloro-2-fluorophenyl)amino)quinazolin-6-yl)-1H-1,2,3-triazol-1-yl)-N-hydroxyhexanamide (9c) Yield 79%; mp 179-181°C; ^{1}H NMR (400 MHz, DMSO) *δ* 12.10 (s, 1H), 10.38 (s, 1H), 9.46 (s, 1H), 8.95 (s, 1H), 8.84 (s, 1H), 8.58 (d, *J* = 8.6 Hz, 1H), 8.05 (d, *J* = 8.7 Hz, 1H), 7.68 (t, *J* = 6.8 Hz, 1H), 7.59 (t, *J* = 6.7 Hz, 1H), 7.40 (t, *J* = 8.1 Hz, 1H), 4.48 (t, *J* = 6.9 Hz, 2H), 2.02 – 1.81 (m, 4H), 1.65 – 1.45 (m, 2H), 1.37 – 1.17 (m, 2H). ^{13}C NMR (101 MHz, DMSO) *δ* 169.40, 161.21, 154.30, 151.81, 151.53, 145.31, 139.13, 133.70, 131.82, 130.11, 128.07, 126.40, 125.89, 125.83, 123.31, 121.54, 121.23, 121.06, 120.89, 114.29, 50.18, 32.53, 29.80, 25.93, 24.97. HR-MS(ESI) *m/z*: Calcd for $[M+H]^+$ 470.1508; Found: 470.1513.

6.1.1.4.

7-(4-(4-((3-chloro-2-fluorophenyl)amino)quinazolin-6-yl)-1H-1,2,3-triazol-1-yl)-N-hydroxyheptanamide (9d) Yield 91%; mp 194-196°C; ^{1}H NMR (400 MHz, DMSO) *δ* 12.25 (s, 1H), 10.39 (s, 1H), 9.56 (s, 1H), 8.95 (s, 1H), 8.88 (s, 1H), 8.60 (dd, *J* = 8.7, 1.4 Hz, 1H), 8.07 (d, *J* = 8.7 Hz, 1H), 7.72 – 7.63 (m, 1H), 7.63 – 7.52 (m, 1H), 7.39 (t, *J* = 8.1 Hz, 1H), 4.47 (t, *J* = 7.0 Hz, 2H), 2.01 – 1.79 (m, 4H), 1.60 – 1.40 (m,

2H), 1.38 – 1.20 (m, 4H). ^{13}C NMR (101 MHz, DMSO) δ 169.53, 161.18, 154.29, 151.80, 151.59, 145.30, 139.21, 133.72, 131.80, 130.10, 128.05, 126.52, 125.91, 125.86, 123.28, 121.62, 121.14, 121.05, 120.89, 114.30, 50.25, 32.63, 29.99, 28.44, 26.06, 25.40. HR-MS(ESI) *m/z*: Calcd for $[M+H]^+$ 484.1664; Found: 484.1660.

6.1.1.5.

6-(4-(4-((3-chloro-4-((3-fluorobenzyl)oxy)phenyl)amino)quinazolin-6-yl)-1H-1,2,3-triazol-1-yl)-N-hydroxyhexanamide (9e) Yield 75%; mp 183-185°C; ^{1}H NMR (400 MHz, DMSO) δ 11.90 (s, 1H), 10.41 (s, 1H), 9.55 (s, 1H), 8.91 (s, 2H), 8.51 (d, J = 8.7 Hz, 1H), 8.04 – 7.90 (m, 2H), 7.71 (dd, J = 8.9, 2.3 Hz, 1H), 7.49 – 7.42 (m, 1H), 7.35 – 7.26 (m, 3H), 7.21 – 7.12 (m, 1H), 5.28 (s, 2H), 4.43 (t, J = 6.8 Hz, 2H), 2.02 – 1.78 (m, 4H), 1.61 – 1.42 (m, 2H), 1.32 – 1.15 (m, 2H). ^{13}C NMR (101 MHz, DMSO) δ 169.41, 163.90, 161.48, 159.98, 152.19, 145.37, 139.92, 139.84, 133.25, 131.57, 131.18, 131.09, 130.90, 126.74, 125.05, 123.87, 123.34, 121.55, 121.08, 115.41, 115.20, 114.68, 114.53, 69.85, 50.14, 32.50, 29.79, 25.90, 24.97. HR-MS(ESI) *m/z*: Calcd for $[M+H]^+$ 576.1926; Found: 576.1919.

6.1.1.6.

7-(4-(4-((3-chloro-4-((3-fluorobenzyl)oxy)phenyl)amino)quinazolin-6-yl)-1H-1,2,3-triazol-1-yl)-N-hydroxyheptanamide (9f) Yield 47%; mp 228-229°C; ^{1}H NMR (400 MHz, DMSO) δ 12.03 (s, 1H), 10.31 (s, 1H), 9.62 (s, 1H), 8.95 (s, 2H), 8.55 (d, J = 8.6 Hz, 1H), 8.10 – 7.91 (m, 2H), 7.74 (d, J = 8.9 Hz, 1H), 7.54 – 7.43 (m, 1H), 7.38 – 7.28 (m, 3H), 7.21 – 7.12 (m, 1H), 5.30 (s, 2H), 4.45 (t, J = 6.1 Hz, 2H), 2.23 – 1.78 (m, 4H), 1.61 – 1.42 (m, 2H), 1.33 – 1.13 (m, 4H). ^{13}C NMR (101 MHz, DMSO)

δ 170.96, 163.90, 161.47, 160.07, 152.26, 145.32, 139.91, 139.83, 133.31, 131.65, 131.18, 131.09, 130.80, 126.83, 125.15, 123.87, 123.38, 121.55, 119.36, 115.41, 115.20, 114.67, 114.52, 69.83, 50.21, 32.62, 29.96, 28.39, 26.06, 25.41. HR-MS(ESI) *m/z*: Calcd for $[M+H]^+$ 590.2083; Found: 590.2073.

6.1.1.7.

6-(4-(4-((3-chloro-4-(thiazol-2-ylmethoxy)phenyl)amino)quinazolin-6-yl)-1H-1,2,3-triazol-1-yl)-N-hydroxyhexanamide (9g) Yield 89%; mp 144-146°C; ^{1}H NMR (400 MHz, DMSO) δ 12.05 (s, 1H), 10.41 (s, 1H), 9.61 (s, 1H), 9.03 – 8.83 (m, 2H), 8.57 (dd, *J* = 8.7, 1.4 Hz, 1H), 8.03 (d, *J* = 8.7 Hz, 1H), 7.99 (d, *J* = 2.5 Hz, 1H), 7.89 (d, *J* = 3.2 Hz, 1H), 7.83 (d, *J* = 3.2 Hz, 1H), 7.75 (dd, *J* = 8.9, 2.5 Hz, 1H), 7.45 (d, *J* = 9.1 Hz, 1H), 5.63 (s, 2H), 4.47 (t, *J* = 6.9 Hz, 2H), 2.03 – 1.81 (m, 4H), 1.63 – 1.46 (m, 2H), 1.36 – 1.19 (m, 2H). ^{13}C NMR (101 MHz, DMSO) δ 169.39, 165.92, 160.22, 151.92, 151.09, 145.32, 143.16, 137.98, 133.52, 131.79, 131.28, 126.94, 125.21, 123.39, 121.93, 121.69, 121.21, 120.70, 114.94, 114.55, 68.17, 50.17, 32.51, 29.79, 25.92, 24.96. HR-MS(ESI) *m/z*: Calcd for $[M+H]^+$ 565.1537; Found: 565.1531.

6.1.1.8.

7-(4-(4-((3-chloro-4-(thiazol-2-ylmethoxy)phenyl)amino)quinazolin-6-yl)-1H-1,2,3-triazol-1-yl)-N-hydroxyheptanamide (9h) Yield 92%; mp 158-160°C; ^{1}H NMR (400 MHz, DMSO) δ 12.02 (s, 1H), 10.42 (s, 1H), 9.61 (s, 1H), 9.07 – 8.83 (m, 2H), 8.56 (dd, *J* = 8.7, 1.4 Hz, 1H), 8.06 – 7.97 (m, 2H), 7.89 (d, *J* = 3.2 Hz, 1H), 7.84 (d, *J* = 3.2 Hz, 1H), 7.78 (dd, *J* = 8.9, 2.4 Hz, 1H), 7.44 (d, *J* = 9.1 Hz, 1H), 5.63 (s, 2H), 4.47 (t, *J* = 6.9 Hz, 2H), 2.01 – 1.80 (m, 4H), 1.62 – 1.41 (m, 2H), 1.39 – 1.17 (m, 4H).

^{13}C NMR (101 MHz, DMSO) δ 169.56, 165.92, 160.08, 151.80, 151.15, 145.35, 143.16, 138.36, 133.32, 131.67, 131.40, 126.81, 125.08, 123.36, 121.91, 121.67, 121.20, 120.94, 114.89, 114.57, 68.17, 50.23, 32.64, 29.96, 28.43, 26.06, 25.40. HR-MS(ESI) *m/z*: Calcd for $[M+H]^+$ 579.1694; Found: 579.1675.

6.1.1.9.

N-hydroxy-6-(4-(4-((3-methyl-4-((6-methylpyridin-3-yl)oxy)phenyl)amino)quinazolin-6-yl)-1H-1,2,3-triazol-1-yl)hexanamide (9i) Yield 55%; mp 133-135°C; ^{1}H NMR (400 MHz, DMSO) δ 12.16 (s, 1H), 10.33 (s, 1H), 9.75 (s, 1H), 9.02 (d, *J* = 6.0 Hz, 1H), 8.96 (s, 1H), 8.59 (d, *J* = 8.6 Hz, 1H), 8.50 (d, *J* = 2.3 Hz, 1H), 8.08 (d, *J* = 8.7 Hz, 1H), 8.01 – 7.91 (m, 1H), 7.84 (s, 1H), 7.79 (d, *J* = 8.8 Hz, 1H), 7.74 (d, *J* = 8.7 Hz, 1H), 7.18 (d, *J* = 8.7 Hz, 1H), 4.47 (t, *J* = 6.6 Hz, 2H), 2.67 (s, 3H), 2.27 (s, 3H), 2.04 – 1.78 (m, 4H), 1.61 – 1.44 (m, 2H), 1.37 – 1.18 (m, 2H). ^{13}C NMR (101 MHz, DMSO) δ 174.85, 169.42, 160.19, 153.83, 151.61, 150.96, 149.70, 145.39, 138.05, 134.11, 133.29, 131.69, 130.02, 128.53, 124.83, 123.49, 120.66, 119.99, 114.55, 50.16, 32.50, 29.77, 25.89, 24.97, 24.39, 16.42. HR-MS(ESI) *m/z*: Calcd for $[M+H]^+$ 539.2519; Found: 539.2510.

6.1.1.10.

N-hydroxy-7-(4-(4-((3-methyl-4-((6-methylpyridin-3-yl)oxy)phenyl)amino)quinazolin-6-yl)-1H-1,2,3-triazol-1-yl)heptanamide (9j) Yield 42%; mp 112-114°C; 1H NMR (400 MHz, DMSO) δ 12.19 (s, 1H), 10.31 (s, 1H), 9.76 (d, *J* = 6.6 Hz, 1H), 9.03 (d, *J* = 6.0 Hz, 1H), 8.97 (s, 1H), 8.60 (d, *J* = 8.7 Hz, 1H), 8.53 (s, 1H), 8.09 (d, *J* = 8.7 Hz, 1H), 8.05 – 7.95 (m, 1H), 7.84 (s, 1H), 7.80 (d, *J* = 8.8 Hz, 1H), 7.74 (d, *J* =

8.7 Hz, 1H), 7.20 (d, *J* = 8.7 Hz, 1H), 4.47 (t, *J* = 6.9 Hz, 2H), 2.69 (s, 3H), 2.27 (s, 3H), 2.00 – 1.77 (m, 4H), 1.60 – 1.40 (m, 2H), 1.37 – 1.20 (m, 4H). ^{13}C NMR (101 MHz, DMSO) δ 174.93, 170.45, 160.23, 151.88, 151.56, 150.98, 148.78, 145.39, 138.04, 134.18, 133.33, 131.72, 130.05, 128.55, 124.87, 123.48, 120.66, 120.04, 114.58, 50.23, 32.62, 29.97, 28.43, 26.06, 25.42, 24.77, 16.42. HR-MS(ESI) *m/z*: Calcd for $[M+H]^+$ 553.2676; Found: 553.2682.

6.1.1.11.

N-hydroxy-6-(4-(4-((3-methoxy-4-phenoxyphenyl)amino)quinazolin-6-yl)-1H-1,2,3-triazol-1-yl)hexanamide (9k) Yield 77%; mp 209-211°C; ^{1}H NMR (400 MHz, DMSO) δ 11.94 (s, 1H), 10.43 (s, 1H), 9.63 (s, 1H), 8.97 (s, 1H), 8.96 (s, 1H), 8.57 (d, *J* = 8.6 Hz, 1H), 8.04 (d, *J* = 8.7 Hz, 1H), 7.72 (d, *J* = 2.1 Hz, 1H), 7.50 (dd, *J* = 8.6, 2.2 Hz, 1H), 7.40 – 7.26 (m, 2H), 7.16 (d, *J* = 8.6 Hz, 1H), 7.06 (t, *J* = 7.3 Hz, 1H), 6.90 (d, *J* = 7.9 Hz, 2H), 4.47 (t, *J* = 6.8 Hz, 2H), 3.78 (s, 3H), 2.04 – 1.80 (m, 4H), 1.62 – 1.36 (m, 2H), 1.38 – 1.17 (m, 2H). ^{13}C NMR (101 MHz, DMSO) δ 169.40, 160.03, 158.20, 151.55, 151.23, 145.39, 142.24, 134.48, 133.30, 131.63, 130.30, 123.40, 122.83, 121.88, 121.11, 117.77, 116.60, 114.65, 110.77, 56.39, 50.14, 32.51, 29.80, 25.90, 24.97. HR-MS(ESI) *m/z*: Calcd for $[M+H]^+$ 540.2359; Found: 540.2362.

6.1.1.12.

N-hydroxy-7-(4-(4-((3-methoxy-4-phenoxyphenyl)amino)quinazolin-6-yl)-1H-1,2,3-triazol-1-yl)heptanamide (9l) Yield 88%; mp 193-195°C; ^{1}H NMR (400 MHz, DMSO) δ 11.95 (s, 1H), 10.39 (s, 1H), 10.24 (s, 1H), 9.59 (s, 1H), 8.98 (s, 1H), 8.93 (s, 1H), 8.57 (d, *J* = 8.8 Hz, 1H), 8.03 (d, *J* = 8.7 Hz, 1H), 7.68 (d, *J* = 2.2 Hz, 1H),

7.47 (dd, *J* = 8.6, 2.4 Hz, 1H), 7.39 – 7.32 (m, 2H), 7.17 (d, *J* = 8.6 Hz, 1H), 7.07 (t, *J* = 7.4 Hz, 1H), 6.90 (d, *J* = 7.8 Hz, 2H), 4.48 (t, *J* = 6.9 Hz, 2H), 3.79 (s, 3H), 1.98 – 1.82 (m, 4H), 1.57 – 1.41 (m, 2H), 1.37 – 1.22 (m, 4H). ^{13}C NMR (101 MHz, DMSO) δ 169.53, 160.13, 158.19, 151.59, 151.21, 145.36, 142.45, 134.38, 133.48, 131.73, 130.29, 123.34, 122.87, 121.85, 121.06, 117.87, 116.67, 114.64, 110.90, 56.44, 50.24, 32.63, 29.98, 28.43, 26.07, 25.40. HR-MS(ESI) *m/z*: Calcd for $[M+H]^+$ 554.2516; Found: 554.2512.

6.2. Bioassay

6.2.1. EGFR and HER2 inhibition assay

In vitro kinase assays were carried out by Medicilon Co., Ltd in Shanghai, China. The general procedures were as the following: 1×kinase buffer was prepared, compounds were transferred to assay plate by echo with 3-fold dilution in 2.5%DMSO/kinase buffer. Then kinases, substrates and compounds in the reaction buffer were mixed. The assay plate was incubated at RT for 15 minutes. ATP was then added to each well to start reaction (positive controls contained gefitinib or lapatinib and all the above components except the inhibitor. The negative controls contained neither enzyme nor inhibitor). The assay plate was incubated at RT for 30 minutes and reaction was stopped by the addition of Streptavidin-XL665 and TK antibody europium cryptate (1:100) solution. The luminescence was monitored at 320 nm (excitation) and 665/615 nm (emission) using an EnVision multilabel plate reader (PerkinElmer Life Sciences, Boston, MA, USA). The signal was correlated with the amount of ATP remaining in the reaction and was inversely correlated with the kinase

activity. The Emission Ratio was calculated with the formula: 665 nm Emission signal/615 nm Emission signal. IC_{50} values were calculated from the inhibitory curves.

6.2.2. HDAC inhibition assay

In vitro HDAC assays were carried out by Shanghai Chempartner Co., Ltd in Shanghai, China. The general procedures were as the following: 1×assay buffer (modified Tris Buffer) was prepared, compounds were transferred to assay plate by echo with 3-fold dilution in 100% DMSO. Substrate solution was made by preparing enzyme solution in 1×assay buffer and adding trypsin and Ac-peptide substrate in 1×assay buffer. Enzyme solution or 1×assay buffer were transferred to assay plate or for low control and incubated at RT for 15 minutes. Substrate solution was then added to each well to start reaction (positive controls contained vorinostat and all the above components except the inhibitor. The negative controls contained neither enzyme nor inhibitor). The plates were incubated for 60 minutes at room temperature to allow the fluorescence signal to develop. The fluorescence generated was monitored at 355 nm (excitation) and 460 nm (emission) using a Synergy MX plate reader (PerkinElmer Life Sciences, Boston, MA, USA). IC_{50} values were calculated from the inhibitory curves.

6.2.3. Cell culture

The human cancer cell lines, A549, A431, BT-474, SK-BR-3 and NCI-H1975 were purchased from American Type Culture Collection (Manassas, VA, USA) and cultured according to the supplier's instructions.

6.2.4. Cytotoxicity assay

Cell viability was assessed by the MTT assay. Briefly, 3-8×10^3 cells were seeded into 96-well plates for 12h, followed by incubation with various doses of compounds for 48 h. After adding 10 μL per well of MTT (5 mg/ml) solution, the formazan crystals were dissolved in 100 μL per well DMSO. The absorbance was measured using Multimode Detector (Beckman Coulter, Fullerton, CA, USA). Three independent experiments were performed.

6.2.5. Western blot analysis

20-40 μg protein was separated by 7.5%-15% SDS-PAGE and transferred to PVDF membrane (Roche). Membranes were blocked for 2h in 1×TBST containing 5% (w/v) BSA, and then incubated with a primary specific antibody in 5% of BSA for 8-12h at 4°C. Followed by a HRP-conjugated anti-mouse or anti-rabbit second antibodies, proteins were visualized with the SuperSignal West Pico Chemiluminescent Substrate kit (Pierce). Antibodies against the following were used: p-EGFR (Tyr1068), p-EGFR (Tyr1173), EGFR, p-HER2 (Tyr1221/1222), p-HER2 (Tyr1248), HER2, Acetyl-Histone H3 (Lys27) were obtained from Cell Signaling Technologies (Cambridge, MA).

6.2.6. Flow cytometry assay

Phosphatidylserine externalization was measured by Annexin V-FITC/PI apoptosis detection kit (Beyotime Company) according to the manufacturer's instructions.

6.2.7. Docking studies

The three-dimensional structure of the EGFR (PDB code: 1XKK) and HDAC2 (PDB code: 4LXZ) were downloaded from RCSB Protein Data Bank. Molecular docking studies were performed by using the SURFLEX-DOCK module of SYBYL program (Tripos, St. Louis, USA) to explore the binding model for the active site pockets of EGFR and HDAC2 with their ligands.[56,57] Hydrogen atoms were added. The general procedure of molecular docking is as followed: (1) ligands and enzymes preparation; (2) protocol generation; (3) docking and scoring; and (4) results analyzing. For molecular modeling, hydrogen atoms were added to the structure. The protonated state of several important residues, such as Met793, Tyr308, Asp181, His145, and His146 were adjusted by using SYBYL program in favor of forming hydrogen bond with the ligand. All atoms located within the range of 5.0 Å from the atoms of the cofactor were selected as the active site, and the corresponding amino acid residue was involved into the active site if any one of its atoms was selected. Other default parameters were adopted in the SURFLEX-DOCK calculations by Silicon Graphics workstation.

Acknowledgments

This work is supported by funding from the National Natural Science Foundation of China (21272134), Shenzhen Municipal Government (CXB201104210014A and 20150113A0410006), and Shenzhen Reform Commission (Disciplinary Development Program for Chemical Biology).

Supplementary data

Supplementary data (synthetic methods and the preparation of compounds **13a-h**,

15a-h, **17a-b**, **18a-b** and **19a-l**, activity and selectivity of small-molecule EGFR/HER2 inhibitors **1-7**) associated with this article can be found in the online version.

References and notes

1. Hynes, N. E.; MacDonald, G. *Curr. Opin. Cell. Biol.* **2009**, *21*, 177.
2. Jin, J.; Pawson, T. *Philos. Trans. R. Soc. Lond. B. Biol. Sci.* **2012**, *367*, 2540.
3. Margolis, B.; Li, N.; Koch, A.; Mohammadi, M.; Hurwitz, D. R.; Zilberstein, A.; Ullrich, A.; Pawson, T.; Schlessinger, J. *EMBO J.* **1990**, *9*, 4375.
4. Roberts, P.; Der, C. *Oncogene* **2007**, *26*, 3291.
5. Engelman, J. A. *Nat. Rev. Cancer* **2009**, *9*, 550.
6. Hynes, N. E.; Lane, H. A. *Nat. Rev. Cancer* **2005**, *5*, 341.
7. Bareschino, M.; Schettino, C.; Troiani, T.; Martinelli, E.; Morgillo, F.; Ciardiello, F. *Ann. Oncol.* **2007**, *18*, vi35.
8. Thatcher, N.; Chang, A.; Parikh, P.; Rodrigues Pereira, J.; Ciuleanu, T.; Von Pawel, J.; Thongprasert, S.; Tan, E. H.; Pemberton, K.; Archer, V. *Lancet* **2005**, *366*, 1527.
9. Wheeler, D. L.; Dunn, E. F.; Harari, P. M. *Nat. Rev. Clin. Oncol.* **2010**, *7*, 493.
10. Pao, W.; Chmielecki, J. *Nat. Rev. Cancer* **2010**, *10*, 760.
11. Sharma, S. V.; Bell, D. W.; Settleman, J.; Haber, D. A. *Nat. Rev. Cancer* **2007**, *7*, 169.
12. Wu, Y.-L.; Zhou, C.; Hu, C.-P.; Feng, J.; Lu, S.; Huang, Y.; Li, W.; Hou, M.; Shi, J. H.; Lee, K. Y.; Xu, C.-R.; Massey, D.; Kim, M.; Shi, Y.; Geater, S. L. *Lancet Oncol.* **2014**, *15*, 213.
13. Cross, D. A. E.; Ashton, S. E.; Ghiorghiu, S.; Eberlein, C.; Nebhan, C. A.; Spitzler, P. J.; Orme, J. P.; Finlay, M. R. V.; Ward, R. A.; Mellor, M. J.; Hughes, G.; Rahi, A.; Jacobs, V. N.; Brewer, M. R.; Ichihara, E.; Sun, J.; Jin, H.; Ballard, P.; Al-Kadhimi, K.; Rowlinson, R.; Klinowska, T.; Richmond, G. H. P.; Cantarini, M.; Kim, D.-W.; Ranson, M. R.; Pao, W. *Cancer Discov.* **2014**, *4*, 1046.
14. Chong, C. R.; Jänne, P. A. *Nat. Med.* **2013**, *19*, 1389.

15. Engelman, J. A.; Zejnullahu, K.; Mitsudomi, T.; Song, Y.; Hyland, C.; Park, J. O.; Lindeman, N.; Gale, C.-M.; Zhao, X.; Christensen, J. *Science* **2007**, *316*, 1039.

16. Al-Lazikani, B.; Banerji, U.; Workman, P. *Nat. Biotechnol.* **2012**, *30*, 679.

17. Taby, R.; Issa, J. P. J. *CA Cancer J. Clin.* **2010**, *60*, 376.

18. Robey, R. W.; Chakraborty, A. R.; Basseville, A.; Luchenko, V.; Bahr, J.; Zhan, Z.; Bates, S. E. *Mol. Pharm.* **2011**, *8*, 2021.

19. Grant, C.; Rahman, F.; Piekarz, R.; Peer, C.; Frye, R.; Robey, R. W.; Gardner, E. R.; Figg, W. D.; Bates, S. E. *Expert Rev. Anticancer Ther.* **2010**, *10*, 997.

20. Ellis, L.; Pan, Y.; Smyth, G. K.; George, D. J.; McCormack, C.; Williams-Truax, R.; Mita, M.; Beck, J.; Burris, H.; Ryan, G. *Clin. Cancer Res.* **2008**, *14*, 4500.

21. Mann, B. S.; Johnson, J. R.; Cohen, M. H.; Justice, R.; Pazdur, R. *Oncologist* **2007**, *12*, 1247.

22. LaBonte, M. J.; Wilson, P. M.; Fazzone, W.; Russell, J.; Louie, S. G.; El-Khoueiry, A.; Lenz, H.-J.; Ladner, R. D. *Cancer Res.* **2011**, *71*, 3635.

23. Edwards, A.; Li, J.; Atadja, P.; Bhalla, K.; Haura, E. B. *Mol. Cancer Ther.* **2007**, *6*, 2515.

24. Bali, P.; Pranpat, M.; Swaby, R.; Fiskus, W.; Yamaguchi, H.; Balasis, M.; Rocha, K.; Wang, H.-G.; Richon, V.; Bhalla, K. *Clin. Cancer Res.* **2005**, *11*, 6382.

25. Scroggins, B. T.; Robzyk, K.; Wang, D.; Marcu, M. G.; Tsutsumi, S.; Beebe, K.; Cotter, R. J.; Felts, S.; Toft, D.; Karnitz, L. *Mol. Cell* **2007**, *25*, 151.

26. Trepel, J.; Mollapour, M.; Giaccone, G.; Neckers, L. *Nat. Rev. Cancer* **2010**, *10*, 537.

27. Whitesell, L.; Lindquist, S. L. *Nat. Rev. Cancer* **2005**, *5*, 761.

28. Mahboobi, S.; Sellmer, A.; Winkler, M.; Eichhorn, E.; Pongratz, H.; Ciossek, T.; Baer, T.; Maier, T.; Beckers, T. *J. Med. Chem.* **2010**, *53*, 8546.

29. Cai, X.; Zhai, H.-X.; Wang, J.; Forrester, J.; Qu, H.; Yin, L.; Lai, C.-J.; Bao, R.; Qian, C. *J. Med. Chem.* **2010**, *53*, 2000.

30. Chen, P. C.; Patil, V.; Guerrant, W.; Green, P.; Oyelere, A. K. *Bioorganic & Medicinal Chemistry* **2008,** *16*, 4839-4853.

31. Tron, G. C.; Pirali, T.; Billington, R. A.; Canonico, P. L.; Sorba, G.; Genazzani, A.

A. *Med. Res. Rev.* **2008**, *28*, 278.

32. Wadsworth, H. J.; Jenkins, S. M.; Orlek, B. S.; Cassidy, F.; Clark, M. S. G.; Brown, F.; Riley, G. J.; Graves, D.; Hawkins, J.; Naylor, C. B. *J. Med. Chem.* **1992**, *35*, 1280.
33. Yun, C.-H.; Boggon, T. J.; Li, Y.; Woo, M. S.; Greulich, H.; Meyerson, M.; Eck, M. J. *Cancer Cell* **2007**, *11*, 217.
34. Wood, E. R.; Truesdale, A. T.; McDonald, O. B.; Yuan, D.; Hassell, A.; Dickerson, S. H.; Ellis, B.; Pennisi, C.; Horne, E.; Lackey, K.; Alligood, K. J.; Rusnak, D. W.; Gilmer, T. M.; Shewchuk, L. *Cancer Res.* **2004**, *64*, 6652.
35. Liao, J. J.-L. *J. Med. Chem.* **2007**, *50*, 409.
36. Finnin, M. S.; Donigian, J. R.; Cohen, A.; Richon, V. M.; Rifkind, R. A.; Marks, P. A.; Breslow, R.; Pavletich, N. P. *Nature* **1999**, *401*, 188.
37. Bhattacharya, S. K.; Cox, E. D.; Kath, J. C.; Mathiowetz, A. M.; Morris, J.; Moyer, J. D.; Pustilnik, L. R.; Rafidi, K.; Richter, D. T.; Su, C.; Wessel, M. D. *Biochem. Biophys. Res. Commun.* **2003**, *307*, 267.
38. Wakeling, A. E.; Guy, S. P.; Woodburn, J. R.; Ashton, S. E.; Curry, B. J.; Barker, A. J.; Gibson, K. H. *Cancer Res.* **2002**, *62*, 5749.
39. Miknis, G.; Wallace, E.; Lyssikatos, J.; Lee, P.; Zhao, Q.; Hans, J.; Topalov, G.; Buckmelter, A.; Tarlton, G.; Ren, L.; Tullis, J.; Bernat, B.; Pieti Opie, L.; Von Carlowitz, I.; Parry, J.; Morales, T.; Perrier, M.; Woessner, R.; Pheneger, T.; Hoffman, K.; Winkler, J.; Koch, K. *Cancer Res.* **2005**, *65*, 801.
40. Rusnak, D. W.; Lackey, K.; Affleck, K.; Wood, E. R.; Alligood, K. J.; Rhodes, N.; Keith, B. R.; Murray, D. M.; Knight, W. B.; Mullin, R. J.; Gilmer, T. M. *Mol. Cancer Ther.* **2001**, *1*, 85.
41. Jani, J. P.; Finn, R. S.; Campbell, M.; Coleman, K. G.; Connell, R. D.; Currier, N.; Emerson, E. O.; Floyd, E.; Harriman, S.; Kath, J. C.; Morris, J.; Moyer, J. D.; Pustilnik, L. R.; Rafidi, K.; Ralston, S.; Rossi, A. M. K.; Steyn, S. J.; Wagner, L.; Winter, S. M.; Bhattacharya, S. K. *Cancer Res.* **2007**, *67*, 9887.
42. Barbacci, E. G.; Pustilnik, L. R.; Rossi, A. M. K.; Emerson, E.; Miller, P. E.; Boscoe, B. P.; Cox, E. D.; Iwata, K. K.; Jani, J. P.; Provoncha, K.; Kath, J. C.; Liu,

Z.; Moyer, J. D. *Cancer Res.* **2003**, *63*, 4450.

43. Lauffer, B. E. L.; Mintzer, R.; Fong, R.; Mukund, S.; Tam, C.; Zilberleyb, I.; Flicke, B.; Ritscher, A.; Fedorowicz, G.; Vallero, R.; Ortwine, D. F.; Gunzner, J.; Modrusan, Z.; Neumann, L.; Koth, C. M.; Lupardus, P. J.; Kaminker, J. S.; Heise, C. E.; Steiner, P. *J. Biol. Chem.* **2013**, *288*, 26926.
44. Hou, J.; Feng, C.; Li, Z.; Fang, Q.; Wang, H.; Gu, G.; Shi, Y.; Liu, P.; Xu, F.; Yin, Z.; Shen, J.; Wang, P. *Eur. J. Med. Chem.* **2011**, *46*, 3190.
45. Hanahan, D. *Lancet* **2013**.
46. Hanahan, D.; Weinberg, R. A. *Cell* **2011**, *144*, 646.
47. Hopkins, A. L. *Nat. Chem. Biol.* **2008**, *4*, 682.
48. Ding, C.; Zhang, C.; Zhang, M.; Chen, Y. Z.; Tan, C.; Tan, Y.; Jiang, Y. *Future Med. Chem.* **2014**, *6*, 1771.
49. Jia, J.; Zhu, F.; Ma, X.; Cao, Z. W.; Li, Y. X.; Chen, Y. Z. *Nat. Rev. Drug Discov.* **2009**, *8*, 111.
50. Anighoro, A.; Bajorath, J.; Rastelli, G. *J. Med. Chem.* **2014**, *57*, 7874.
51. Peters, J.-U. *J. Med. Chem.* **2013**, *56*, 8955.
52. Guerrant, W.; Patil, V.; Canzoneri, J. C.; Oyelere, A. K. *J. Med. Chem.* **2012**, *55*, 1465.
53. Gryder, B. E.; Sodji, Q. H.; Oyelere, A. K. *Future Med. Chem.* **2012**, *4*, 505.
54. Gryder, B. E.; Rood, M. K.; Johnson, K. A.; Patil, V.; Raftery, E. D.; Yao, L.-P. D.; Rice, M.; Azizi, B.; Doyle, D. F.; Oyelere, A. K. *Journal of Medicinal Chemistry* **2013,** *56*, 5782-5796.
55. Costantino, L.; Barlocco, D. *Future Med. Chem.* **2012**, *5*, 5.
56. Zhang, X.; Peng, T.; Ji, X.; Li, J.; Tong, L.; Li, Z.; Yang, W.; Xu, Y.; Li, M.; Ding, J.; Jiang, H.; Xie, H.; Liu, H. *Bioorg. Med. Chem.* **2013**, *21*, 7988.
57. Tu, Y.; OuYang, Y.; Xu, S.; Zhu, Y.; Li, G.; Sun, C.; Zheng, P.; Zhu, W. *Bioorg. Med. Chem.* **2016**, *24*, 1495.

Captions

Scheme 1. Design strategy of novel EGFR/HER2/HDAC multitarget inhibitors.

Scheme 2. Reagents and conditions: (a) NH_2CHO, reflux; (b) $SOCl_2$, DMF(cat), reflux; (c) anilines, iso-PrOH, 80°C; (d) trimethylsilylacetylene, $Pd(PPh_3)_2Cl_2$, CuI, THF/Et_3N, 80°C; (e) TBAF, THF, RT; (f) NaN_3, DMF, 80°C; (g) NH_2OTHP, EDCI, DMAP, $CHCl_3$, RT; (h) $CuSO_4 \cdot 5H_2O$, sodium ascorbate, DMF, 60°C; (i) HCl, dioxane, RT.

Figure 1. Selected quinazoline-based EGFR/HER2 inhibitors **1-6**, EGFR/HER2/HDAC multitarget inhibitor **7** and HDAC inhibitor **8**.

Figure 2. (A) Western blot analysis of A549 cells treated for 24 h with compound **9d**, (B) Western blot analysis of BT-474 cells treated for 24 h with compound **9d**.

Figure 3. *In vitro* apoptosis analysis of **9d** in BT-474 cells.

Figure 4. (A) Proposed binding mode of compounds **9d** with EGFR (1XKK), (B) Proposed binding mode of compounds **9d** with HDAC2 (4LXZ) (N and O atoms in blue and red, respectively). These images were generated using the SYBYL program.

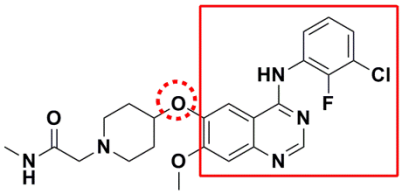

Sapitinib (AZD-8931)
EGFR/HER2 inhibitor

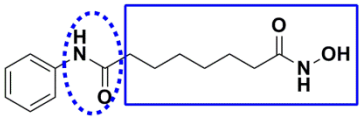

Vorinostat (SAHA)
HDAC inhibitor

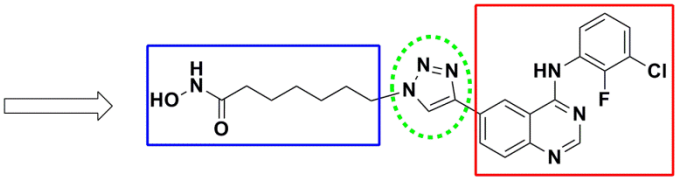

9d
EGFR/HER2/HDAC multitarget inhibitor

- 6-(1,2,3-triazol-4-yl)-4-aminoquinazolins were designed and synthesized.
- Final compounds displayed outstanding inhibitory activity on EGFR, HER2 and HDAC.
- Compounds **9b** and **9d** showed potent activity against five cancer cell lines.
- Compound **9d** regulated the cellular level of p-EGFR, p-HER2 and histone H3.
- Compound **9d** induced remarkable apoptosis in BT-474 cells.